Turk J Chem
35 (2011) , 573 – 585.

doi:10.3906/kim-1007-784

Simultaneous determination of dopamine, uric acid, and folic acid by a modified TiO_2 nanoparticles carbon paste electrode

Mohammad MAZLOUM ARDAKANI[1,*], Mohammad Ali SHEIKH MOHSENI[1], Hadi BEITOLLAHI[1], Ali BENVIDI[1], Hossein NAEIMI[2]

[1] *Department of Chemistry, Faculty of Science, Yazd University, Yazd, 89195-741, I.R.-IRAN*

e-mail: mazloum@yazduni.ac.ir

[2] *Department of Organic Chemistry, Faculty of Chemistry, University of Kashan, Kashan, I.R.-IRAN*

Received: 09.07.2010

The electrochemical behavior of dopamine (DA) was studied at the surface of a 2,2-[1,2 buthanediylbis(nitriloethylidyne)]-bis-hydroquinone/TiO_2 nanoparticles modified carbon paste electrode (BQTMCPE) in aqueous media using voltammetric and chronoamperometric techniques. It was found that under optimum conditions (pH 8.0), the oxidation of DA at the surface of such an electrode occurred at about 220 mV lower than that of an unmodified carbon paste electrode (CPE). Using differential pulse voltammetry (DPV), a highly selective and simultaneous determination of DA, uric acid (UA), and folic acid (FA) was explored at the modified electrode. DPV peak currents of DA, UA, and FA increased linearly with their concentrations in the ranges of 1.0-900.0 μM, 200.0-1500.0 μM, and 200.0-2700.0 μM, respectively, and the detection limits for DA, UA, and FA were 0.3 μM, 12.0 μM, and 32.0 μM, respectively. This method was also used for the determination of DA in pharmaceutical preparation (DA injection) by the standard addition method.

Key Words: Modified electrode, dopamine, uric acid, folic acid, TiO_2 nanoparticles

Introduction

The unique chemical and physical properties of nanoparticles make them extremely suitable for designing new and improved sensing devices, especially electrochemical sensors and biosensors. Many kinds of nanoparticles,

*Corresponding author

such as metal, oxide, and semiconductor nanoparticles, have been used for constructing electrochemical sensors and biosensors, and these nanoparticles play different roles in different sensing systems. The important functions provided by nanoparticles include the immobilization of biomolecules, the catalysis of electrochemical reactions, the enhancement of electron transfer between electrode surfaces and proteins, the labeling of biomolecules, and even the ability to act as a reactant.[1−3]

The trace DA assay is an important neurotransmitter in the mammalian central nervous system. It can cause Parkinson's disease and other similar diseases.[4] Thus, various commonly usable analytical methods for DA and its analogs have been developed in the past. Some examples of these methods are rapid liquid chromatography/tandem mass spectrometry (LC-MS/MS),[5] the chromatography method,[6] the capillary electrophoresis mass spectrometry method, and the fluorescence method.[7] These methods are very sensitive. All of these techniques, however, require a compressing system, temperature controlling systems, separation systems, and other spectrophotometric or electric detection systems. Recently, there has been an increasing demand for more sensitive and simple analytical methods. Voltammetric techniques are very useful and popular for trace analysis, since these techniques are compact, efficient, and sensitive.[8] Various voltammetry solutions have been found to have the low detection limit required for neurotransmitter DA analysis, depending on the working electrode systems.[9,10]

Uric acid (UA) is a primary end product of purine metabolism. Abnormal levels of UA are symptoms of several diseases, such as gout, hyperpiesia, and Lesch-Nyhan syndrome.[11] Hence, monitoring of the concentration of UA in biological fluids may be used as an early warning of the presence of these diseases. Colorimetric, enzymatic, and electrochemical methods are used to determine the concentration of UA.[12,13] The colorimetric method is unreliable for accurate determination of the concentration of UA. Although determination of UA by enzymatic methods is promising due to their high level of selectivity, this methodology is inherently expensive and does not have a high detection limit. Electrochemical methods for the determination of UA are more selective, less expensive, and less time-consuming than the other methods.[14]

Folic acid (FA) is a water-soluble B vitamin that helps build healthy cells. Deficiency of FA is a common cause of anemia and is thought to increase the likelihood of heart attack and stroke. Many studies suggest that diminished folate status is associated with enhanced carcinogenesis, as FA, along with vitamin B_{12}, participates in nucleotide synthesis, cell division, and gene expression.[15] Periconceptual supplementation of FA has been demonstrated to significantly reduce the incidence and reoccurrence of neural tube defects, such as spina bifida of women.[16] A survey of the literature reveals that there are various methods available for the determination of FA, which include liquid chromatography,[17] high performance liquid chromatography,[18] flow-injection chemiluminometry,[19] isotope dilution-liquid chromatography/tandem mass spectrometry,[20] and spectrophotometric methods.[21] As FA is an electroactive component, some electrochemical methods have been reported for its determination.[22] Compared with other technologies, the electrochemical method is more desirable because of its convenience and low cost.

Electrochemical methods traditionally have found important applications in sample analysis and in organic and inorganic synthesis. The electrode surface itself can be a powerful tool in such applications.[23] Apart from the conventional electrodes such as Au, Hg, and Pt, carbon is a preferred substrate in electroanalytical studies.[24] Biological fluids and organic or inorganic substances are best determined at modified carbon electrodes and also at modified carbon paste electrodes.[25−27] The overpotential phenomena make most of the

clinically important compounds difficult to analyze at conventional electrodes, which is promoted by incorporating redox mediators by various methods.[28] There are 4 principle enhancement techniques for voltammetric and amperometric electrodes, namely selective preconcentration, permselectivity, selective recognition, and electrocatalysis.[29]

To our knowledge, no study has reported the electrocatalytic and simultaneous determination of DA, UA, and FA by using TiO_2 modified carbon paste electrodes. Thus, in the present work, we described the preparation and suitability of a BQTMCPE as a new electrode in the electrocatalysis and determination of DA in an aqueous buffer solution, and then we evaluated the analytical performance of the modified electrode in quantification of DA in the presence of UA and FA.

Experimental

Apparatus and chemicals

A potentiostat/galvanostat (SAMA 500, electroanalyzer system, I.R. Iran) was used to carry out the electrochemical experiments. A conventional 3-electrode cell was used at 25 ± 1 °C. A saturated calomel electrode, platinum wire, and BQTMCPE were used as reference, auxiliary, and working electrodes, respectively. A Metrohm model 691 pH/mV meter was also used for pH measurements.

All solutions were freshly prepared with doubly distilled water. DA, UA, FA, and other reagents were of analytical grade (Merck). Graphite powder (Merck) and paraffin oil (DC 350, Merck, density = 0.88 g cm^{-3}) were used as binding agents for graphite pastes. Buffer solutions were prepared from orthophosphoric acid, and its salts were in the pH range of 2.0-12.0. TiO_2 nanoparticles and BQ were synthesized in our laboratory.

A colloidal suspension of TiO_2 nanoparticles was synthesized by mixing titanium tetraisopropoxide, H_2O_2, and H_2O with volume proportions of 12:90:200, respectively. The resulting solution was refluxed for 10 h to promote the crystallinity (surface area = 84 m^2 g^{-1}, particle size = 6.7 nm).

Preparation of the electrode

Carbon nanoparticles paste electrodes were prepared by dissolving BQ in CH_3Cl and hand-mixing it with graphite powder and TiO_2 nanoparticles using a mortar and pestle, with a flowing weight percentage of 1:95:4%, respectively. Paraffin was added to the above mixture and mixed for 20 min until a uniformly wetted paste was obtained. This paste was then packed into the end of a glass tube (approximately 3.6 mm i.d. and 10 cm long). A copper wire inserted into the carbon paste provided an electrical contact. When necessary, a new surface was obtained by pushing an excess of paste out of the tube, which was then polished with weighing paper. BQ-modified CPE (BQMCPE) and TiO_2 nanoparticles CPE (TCPE) were prepared in the same way, without the adding of TiO_2 nanoparticles and BQ, respectively. Unmodified carbon paste electrode (CPE) was also prepared in the same way, without adding BQ or TiO_2 nanoparticles to the mixture. These were used for comparison purposes.

Results and discussion

Electrochemistry of BQTMCPE

Based on our knowledge, there has not been a prior report on the electrochemical properties and, in particular, the electrocatalytic activity of BQ in aqueous media. This compound is insoluble in aqueous media; therefore, we prepared a BQTMCPE and studied its electrochemical properties in a buffered aqueous solution (pH 8.0) using cyclic voltammetry. Cyclic voltammograms of BQ in the BQTMCPE exhibited an anodic and corresponding cathodic peak, whereas cyclic voltammograms of unmodified carbon paste electrodes in a supporting electrolyte showed no anodic or cathodic peaks. Experimental results showed well-defined and reproducible anodic and cathodic peaks (with E_{pa} = 0.18 V, E_{pc} = 0.09 V, $E_{1/2}$ = 0.135 V versus SCE, and ΔE_p = 0.09 V) for BQ; therefore, this substance can be used as a mediator for the electrocatalysis of some important biological compounds with slow electron transfer.

The peak separation potential, $\Delta E_p = (E_{pa} - E_{pc})$, was greater than the 59/n mV expected for a reversible system. This result suggests that the redox couple in the BQTMCPE shows quasireversible behavior in an aqueous medium.

In addition, the effect of the potential scan rate on electrochemical properties of the BQTMCPE was studied in an aqueous solution with cyclic voltammetry. Plots of the anodic and cathodic peak currents (I_p) were linearly dependent on ν at scan rates from 20 to 700 mV s^{-1}. A linear correlation was obtained between peak currents, and the scan rate indicates that the nature of the redox process was controlled in a diffusionless manner (Figure 1A).

The apparent charge transfer rate constant, k_s, and the charge transfer coefficient, α, of a surface-confined redox couple can be evaluated from cyclic voltammetric experiments and by using the variation of anodic and cathodic peak potentials with the logarithm of the scan rate, according to the procedure of Laviron.[30] Figure 1B shows the variations of peak potentials (E_p) as a function of the logarithm of the potential scan rate. We found that the E_p values were proportional to the logarithm of the potential scan rate for scan rates higher than 1000 mV s^{-1} (Figure 1B). The slopes of Figure 1B can be used to extract the kinetic parameters α_c (cathodic transfer coefficient) and α_a (anodic transfer coefficient). The slope of the linear segment is equal to -2.303RT/αnF and 2.303RT/(1 - α)nF for the cathodic and anodic peaks, respectively. The evaluated value for the anodic transfer coefficient (α_a) is 0.36.

The following equation can be used to determine the electron transfer rate constant between the modifier (BQ) and CPE:

$$\log k_s = \alpha \log(1-\alpha) + (1-\alpha)\log\alpha - \log(RT/nF\nu) - \alpha(1-\alpha)nF\Delta E_p/2.3RT, \quad (1)$$

where (1-α)n_α = 0.64, v is the sweep rate, and all other symbols have their conventional meanings. The value of k_s = 13.0 ± 0.6 s^{-1} was evaluated using Eq. (1).

An approximate estimate of the surface coverage of the electrode was made by adopting the method used by Sharp.[31] According to this method, the peak current is related to the surface concentration of the electroactive species, Γ, by the following equation:

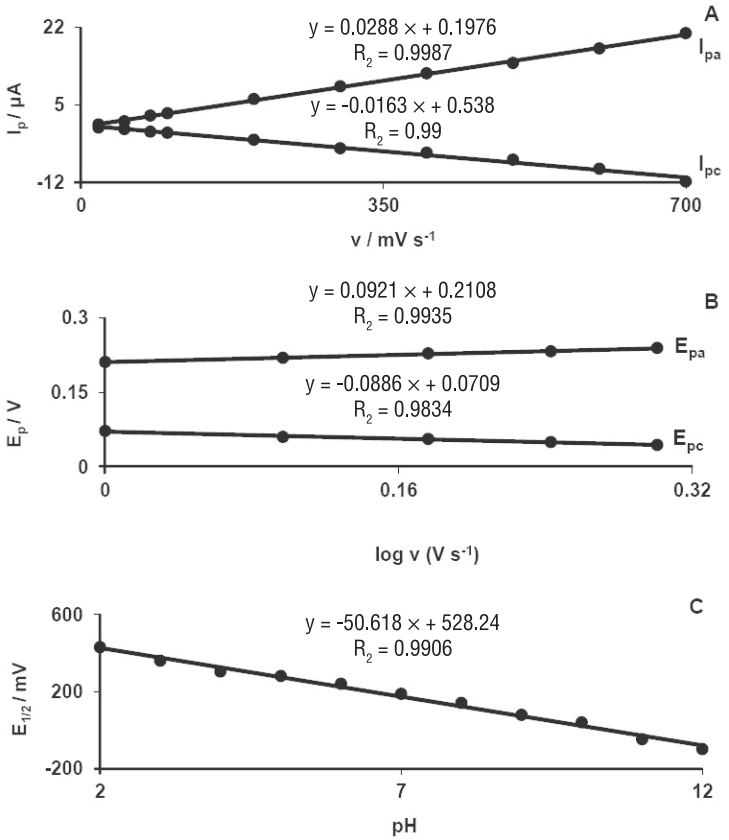

Figure 1. A) Variations of I_p versus different scan rates: 20, 50, 80, 100, 200, 300, 400, 500, 600, and 700 mV s^{-1}. B) Variation of E_p versus the logarithm of the high scan rate: 1000, 1250, 1500, 1750, and 2000 mV s^{-1}. C) Variation of $E_{1/2}$ versus the various buffered pH levels: 2.0, 3.0, 4.0, 5.0, 6.0, 7.0, 8.0, 9.0, 10.0, 11.0, and 12.0.

$$I_p = n^2F^2A\Gamma\nu/4RT, \tag{2}$$

where n represents the number of electrons involved in the reaction, A is the surface area (0.0962 cm^2) of the BQTMCPE, Γ (mol cm^{-2}) is the surface coverage, and the other symbols have their usual meanings. From the slope of the anodic peak currents versus the scan rate (Figure 1A), the calculated surface concentration of BQ is $= 7.8 \times 10^{-11}$ mol cm^{-2} for n = 2.

The electrochemical response of the BQ molecule is generally pH-dependent. Thus, the electrochemical behavior of the BQTMCPE was studied at different pH levels using cyclic voltammetry. Anodic and cathodic peak potentials of the BQTMCPE were shifted to less positive values with increases in pH. The half-wave potential of the BQTMCPE at various pH levels was calculated as the average value of the anodic and cathodic peak potentials of the CVs. A potential-pH diagram was constructed by plotting the calculated $E_{1/2}$ values as a function of pH (Figure 1C). This diagram is composed of a straight line with a slope of 50.61 mV pH^{-1}. Such behavior suggests that it obeys the Nernst equation for a 2-electron and proton transfer reaction.[32]

Electrocatalytic oxidation of DA at a BQTMCPE

Electrocatalytic oxidation of DA at a BQTMCPE can be seen in Figure 2. This figure depicts the cyclic voltammetric responses from the electrochemical oxidation of 0.2 mM DA at the BQTMCPE (curve f), BQ-modified CPE (BQMCPE) (curve e), TiO_2 nanoparticles CPE (TCPE) (curve d), and unmodified CPE (curve a). As shown, the anodic peak potential for DA oxidation at the BQTMCPE (curve f) and BQMCPE (curve e) was about 180 mV, while at the TCPE (curve d), the peak potential was about 330 mV. At the unmodified CPE, the peak potential was about 400 mV of DA (curve b). From these results, it was concluded that the best electrocatalytic effect for DA oxidation was observed at the BQTMCPE (curve f). For example, results show that the peak potential of DA oxidation at the BQTMCPE (curve f) shifted by about 150 and 220 mV toward negative values when compared with that at the TCPE (curve d) and unmodified carbon paste electrode (curve b), respectively.

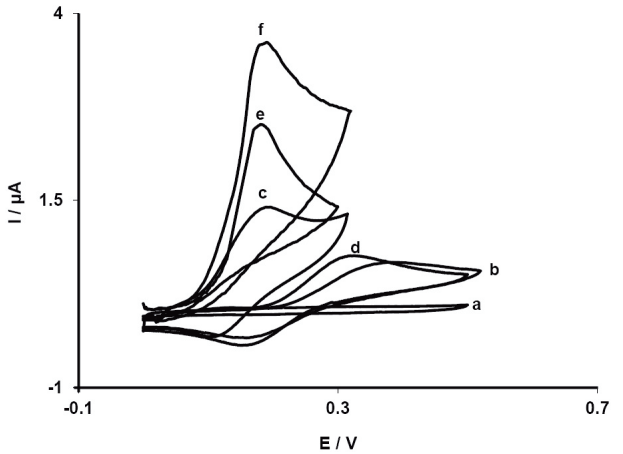

Figure 2. Cyclic voltammograms of 0.2 mM DA at the (b) unmodified CPE, (d) TCPE, (e) BQMCPE, and (f) BQTMCPE. (a) and (c) show the CVs of blank solution at the unmodified CPE and BQTMCPE, respectively. Electrolyte: 0.1 M phosphate buffer solution (pH 8.0), scan rate: 10 mV s^{-1}.

Similarly, when comparing the oxidation of DA at the BQMCPE (curve e) and BQTMCPE (curve f), a dramatic enhancement of the anodic peak current at the BQTMCPE relative to that obtained at the BQMCPE was observed. In other words, the data clearly show that the combination of TiO_2 nanoparticles and mediator BQ definitely improved the characteristics of DA oxidation. The BQTMCPE, in 0.1 M phosphate buffer (pH 8.0) and without DA in solution, exhibited a well-behaved redox reaction (curve c); upon addition of 0.2 mM DA there was a dramatic enhancement of the anodic peak current (curve f), indicating a strong electrocatalytic effect.[32]

The effect of scan rate on the electrocatalytic oxidation of DA at the BQTMCPE was investigated by cyclic voltammetry (Figure 3A). As can be observed in Figure 3, the oxidation peak potential shifted with increasing scan rates toward a more positive potential, confirming the kinetic limitation of the electrochemical reaction. A plot of peak height (I_p) versus the square root of the scan rate ($\nu^{1/2}$), in the range of 2-30 mV s^{-1}, was also constructed (Figure 3A, inset a). This plot was found to be linear, suggesting that, at sufficient overpotential, the process was diffusion- rather than surface-controlled. A plot of the sweep rate-normalized

current ($I_p/\nu^{1/2}$) versus sweep rate (Figure 3A, inset b) exhibits the characteristic shape of an EC process.[32]

Figure 3B shows a Tafel plot that was drawn from data of the rising part of the current-voltage curve recorded at a scan rate of 10 mV s^{-1}. This part of the voltammogram, known as the Tafel region, is affected by electron transfer kinetics between the substrate (DA) and surface-confined BQ, assuming the deprotonation of the substrate as a sufficiently fast step. In this condition, the number of electrons involved in the rate-determining step can be estimated from the slope of the Tafel plot. A slope of 0.106 V $decade^{-1}$ was obtained, indicating a one-electron transfer to be rate-limiting assuming a transfer coefficient of $\alpha = 0.45$.

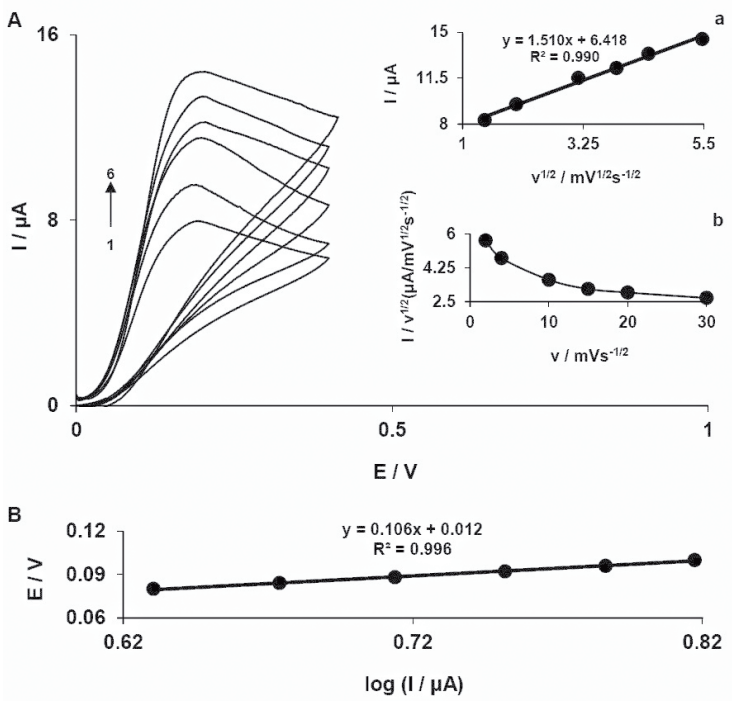

Figure 3. A) Cyclic voltammograms of a BQTMCPE in 0.1 M phosphate buffer (pH 8.0) containing 0.5 mM DA at different scan rates; the numbers 1 to 6 correspond to 2, 4, 10, 15, 20, and 30 mV s^{-1} scan rates. Insets: (a) Variation of the electrocatalytic currents versus the square root of the scan rate, (b) variation of the scan rate-normalized current ($I_p/\nu^{1/2}$) with scan rate. B) Tafel plot derived from the rising part of the voltammogram recorded at a scan rate of 10 mV s^{-1}.

Chronoamperometric measurements

Chronoamperometry, as well as the other electrochemical methods, was employed for the investigation of electrode processes at chemically modified electrodes. Figure 4A shows the chronoamperometric measurements of DA at the BQTMCPE. This figure represents the current-time profiles obtained by setting the working electrode potential to 400 mV for various concentrations of DA. For an electroactive material (DA, in this case) with a diffusion coefficient of D, the current for the electrochemical reaction (at a mass transport limited rate) is described by the Cottrell equation.[32] Under diffusion control, a plot of I versus $t^{-1/2}$ will be linear, and from

the slope, the value of D can be obtained. Inset (a) of Figure 4A shows the experimental plots with the best fits for the different concentrations of DA employed. The slopes of the resulting straight lines were plotted versus the DA concentration (Figure 4A inset b). The value of D was found to be 2.8×10^{-5} cm^2 s^{-1}.

Chronoamperometry can also be employed to evaluate the catalytic rate constant, k, for the reaction between DA and the BQTMCPE according to the method of Galus:[33]

$$I_C/I_L = \pi^{1/2}\gamma^{1/2} = \pi^{1/2}(kC_bt)^{1/2}, \tag{3}$$

where I_C is the catalytic current of DA at the BQTMCPE, I_L is the limited current in the absence of DA, $\gamma = kC_bt$, t is the time elapsed, and C_b is the bulk concentration of DA. The above equation can be used to calculate the rate constant of the catalytic process k. Based on the slope of the I_C/I_L versus $t^{1/2}$ plot, k can be obtained for a given DA concentration. Such plots obtained from the chronoamperograms in Figure 4 are shown in Figure 4B. From the values of the slopes, the average value of k was found to be $k = 3.1 \times 10^5$ M^{-1} s^{-1}.

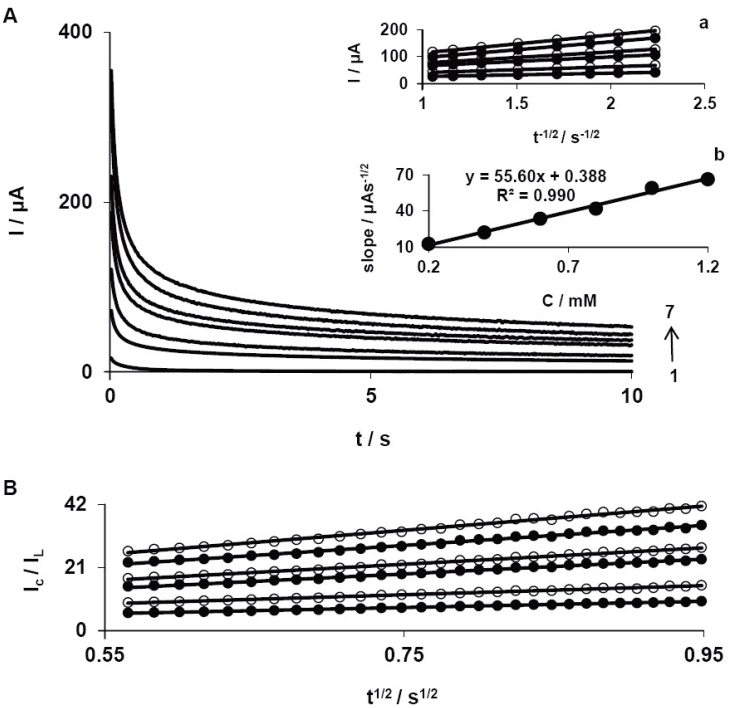

Figure 4. A) Chronoamperograms obtained at BQTMCPE in 0.1 M phosphate buffer solution (pH 8.0) for different concentrations of DA. The numbers 1 to 7 correspond to 0.0, 0.2, 0.4, 0.6, 0.8, 1.0, and 1.2 mM DA. Insets: (a) plots of I vs. $t^{-1/2}$ obtained from chronoamperograms 2-7, (b) plot of the slope of the straight lines against the DA concentration. B) Dependence of I_{cat}/I_l on $t^{1/2}$ derived from the data of the chronoamperograms.

The value of k also explains the sharp feature of the catalytic peak observed for the catalytic oxidation of DA at the surface of the BQTMCPE. Finally, the heterogeneous rate constant (k′) of catalytic reaction was calculated as $k' = 2.42 \times 10^{-2}$ cm s^{-1}.

Calibration plot and limit of detection

Differential pulse voltammetry was used to determine the concentration of DA. Voltammograms clearly showed that the plot of peak current versus DA concentration consisted of 2 linear segments with different slopes, 0.5215 μA μM^{-1} for the first linear segment and 0.0373 μA μM^{-1} for the second linear segment, corresponding to 2 different ranges of substrate concentrations, 1.0-8.0 μM for the first linear segment and 8.0-900.0 μM for the second linear segment. The decrease of sensitivity (slope) in the second linear range is likely to be due to kinetic limitation. The detection limit (3σ) for DA in the lower range region was found to be 0.3 μM. This value is comparable with values reported by other researchers (Table 1). As can be seen from Table 1, different parameters of BQTMCPE for electrocatalytic oxidation of DA are better than results from other works.

Simultaneous determination of DA, UA, and FA

The main objective of this study was to detect DA, UA, and FA simultaneously. The utilization of the BQTMCPE for the simultaneous determination of DA, UA, and FA was demonstrated by simultaneously changing the concentrations of DA, UA, and FA. The DP voltammetric results showed that the simultaneous determination of DA, UA, and FA with 3 well-distinguished anodic peaks at potentials of 90, 420, and 760 mV, corresponding to the oxidation of DA, UA, and FA, respectively, could be possible at the BQTMCPE (Figure 5). By contrast, the bare electrode could not separate the voltammetric signals of these substances and an overlapped voltammogram was obtained for the analytes.

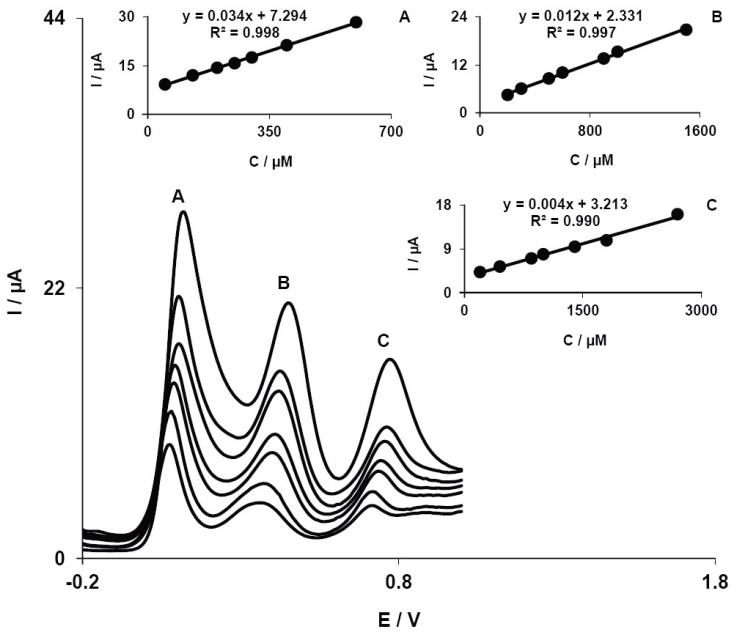

Figure 5. Differential pulse voltammograms of BQTMCPE in 0.1 M phosphate buffer solution (pH 8.0) containing different concentrations of DA, UA, and FA (from inner to outer) mixed solutions of 50.0 + 200.0 + 200.0, 130.0 + 300.0 + 450.0, 200.0 + 500.0 + 850.0, 250.0 + 600.0 + 1000.0, 300.0 + 900.0 + 1400.0, 400.0 + 1000.0 + 1800.0, and 600.0 + 1500.0 +2700.0, respectively, in which the first value is the concentration of DA in μM, the second value is the concentration of UA in μM, and the last value is the concentration of FA in μM. Insets: plots of the peak currents as a function of (A) DA, (B) UA, and (C) FA concentration, respectively.

Table 1. Comparison of the efficiency of some modified electrodes used in the electrocatalysis of DA.

Electrode	Modifier	Method	pH	Peak potential shift (mV)	Scan rate ($mV\ s^{-1}$)	Limit of detection (M)	Dynamic range (M)	Reference
Carbon paste	Ionic liquid	Voltammetry	6.8	135	50	1.0×10^{-6}	2.0×10^{-6}–1.5×10^{-3}	34
Glassy carbon	Poly(eriochrome black T)	Voltammetry	4.0	204	100	2.0×10^{-8}	1.0×10^{-7}–2.0×10^{-4}	35
Glassy carbon	Fc-SWNT	Voltammetry	7.0	300	50	5.0×10^{-8}	5.0×10^{-6}–3.0×10^{-5}	36
Glassy carbon	Poly-chromotrope 2B	Voltammetry	5.0	-	100	3.0×10^{-7}	2.0×10^{-6}–8.0×10^{-5}	37
Glassy carbon	Thionine	Voltammetry	4.0	-	50	8.0×10^{-8}	1.0×10^{-7}–8.0×10^{-5}	38
TiO_2 carbon paste	BQ	Voltammetry	8.0	220	10	3.0×10^{-7}	1.0×10^{-6}–9.0×10^{-4}	This work

The sensitivity of the modified electrode toward the oxidation of DA was found to be 0.0349 μA μM^{-1}, whereas the sensitivity toward DA in the absence of UA and FA was found to be 0.0370 μA μM^{-1}. It is very interesting to note that the sensitivities of the modified electrode toward DA in the absence and presence of UA and FA were virtually the same, which indicates the fact that the oxidation processes of DA, UA, and FA at the BQTMCPE were independent; therefore, simultaneous or independent measurements of the 3 analytes are possible without any interference. If the DA signal were affected by the UA or FA, the above-mentioned slopes would be different.

Analytical applications

To evaluate the applicability of the proposed method, the recovery of DA was determined for DA injection. With a phosphate buffer solution (0.1 M, pH 8.0), 1 mL of the DA ampoule was diluted to 50 mL; then 0.5 mL of this solution was diluted to 10 mL and transferred to the voltammetric cell for the voltammetric determinations. The potential was controlled between 0 and 0.2 V at 10 mV s^{-1}. The I_{pa} was measured at the oxidation potential of DA. The amount of DA in the injection was determined, which corresponded quite well with the specified value. This procedure was repeated 5 times on 2 different injection samples and the relative standard deviation was obtained in each case (Table 2).

Table 2. Determination of DA in DA injection.

Sample of DA injection (Real value (mg))	Number of experiment and measured value (mg) ± SD				
	1	2	3	4	5
Number 1 (40)	38.5 ± 1.5	38.2 ± 1.9	38.8 ± 1.8	38.5 ± 1.5	38.5 ± 1.6
Number 2 (40)	39.0 ± 1.1	39.5 ± 0.9	39.1 ± 1.1	38.9 ± 1.3	39.0 ± 1.0

Conclusions

A carbon paste electrode modified with BQ and TiO_2 nanoparticles was fabricated and used for electrocatalytic determination of DA. The results demonstrated that the electrooxidation of DA at the surface of the BQTMCPE occurred at a potential about 220 mV less positive than that of the bare carbon paste electrode. The application of BQTMCPE for the simultaneous determination of DA, UA, and FA was demonstrated. The detected potential differences of 330, 670, and 340 mV between DA-UA, DA-FA, and UA-FA, respectively, were large enough to determine DA, UA, and FA individually and simultaneously. Finally, this electrode was used for the determination of DA in DA injection using the standard addition method.

Acknowledgements

The authors would like to thank Yazd University Research Council, IUT Research Council, and Excellence in Sensors for financial support of this research. We gratefully acknowledge Dr. N. Taghavinia of Sharif University of Technology for synthesis of the nanoparticles.

References

1. Beitollahi, H.; Mazloum-Ardakani, M.; Ganjipour, B.; Naeimi, H. *Biosens. Bioelectron.* **2008**, *24*, 362–368.
2. Tabeshnia, M.; Heli, H.; Jabbari, A.; Moosavi-Movahedi, A. A. *Turk. J. Chem.* **2010**, *34*, 35–45.
3. Mazloum-Ardakani, M.; Beitollahi, H.; Taleat, Z.; Naeimi, H.; Taghavinia, N. *J. Electroanal. Chem.* **2010**, *644*, 1–6.
4. Xu, F.; Gao, M.; Wang, L.; Shi, G.; Zhang, W.; Jin, L.; Jin, J. *Talanta* **2001**, *55*, 329–336.
5. Hows, M. E. P.; Lacroix, L.; Heidbreder, C.; Organ, A. J.; Shah, A. J. *J. Neuroscience Methods* **2004**, *138*, 123–132.
6. Sabbioni, C.; Saracino, M. A.; Mandrioli, R.; Pinzauti, S.; Furlanetto, S.; Gerra, G.; Raggi, M. A. *J. Chromatogr. A* **2004**, *1081*, 65–71.
7. Peterson, Z. D.; Collins D. C. *J. Chromatogr. B* **2002**, *776*, 221–229.
8. Wang, J.; Serra, B.; Ly, S. Y.; Lu, J.; Pingarron, J. M. *Talanta* **2001**, *54*, 147–151.
9. Mazloum-Ardakani, M.; Beitollahi, H.; Ganjipour, B.; Naeimi, H.; Nejati, M. *Bioelectrochemistry* **2009**, *75*, 1–8.
10. Erdoğdu, G.; Karagözler, A. E. *Turk. J. Chem.* **2007**, *31*, 171–178.
11. Haper, H. A. *Review of Physiological Chemistry*, 16th ed., Lange Medical Publications, San Francisco, CA, 1977.
12. Wyngaarden, B. J.; Kelly, N. W. *Gout and Hyperuricemia*, Grune and Stratton, New York, 1974.
13. Cunningham, S. K.; Keaveny, T. V. *Clin. Chim. Acta* **1978**, *86*, 217–221.
14. Beitollahi, H.; Mazloum-Ardakani, M.; Naeimi, H.; Ganjipour, B. *J. Solid State Electrochem.* **2009**, *13*, 353–363.
15. Hoegger, D.; Morier, P.; Vollet, C.; Heini, D.; Reymond, F.; Rossier, J. S. *Anal. Bioanal. Chem.* **2007**, *387*, 267–275.
16. Gujska, E.; Kuncewicz, A. *Eur. Food Res. Technol.* **2005**, *221*, 208–213.
17. Holcomb, I. J.; Fusari, S. A. *Anal. Chem.* **1981**, *53*, 607–609.
18. Gregory, J. F.; Day, B. P. F.; Ristow, K. A. *J. Food Sci.* **1982**, *47*, 1568–1571.
19. Alwarthan, A. A. *Anal. Sci.* **1994**, *10*, 919–922.
20. Jung, M.; Kim, B.; Boo, D. W.; So, H. Y. *Bull. Korean Chem. Soc.* **2007**, *28*, 745.
21. Ganguly, S. K.; Bhattachary, H. *Ind. J. Pharm. Sci.* **1957**, *19*, 170–173.
22. Mazloum-Ardakani, M.; Beitollahi, H.; Sheikh-Mohseni, M. A.; Naeimi, H.; Taghavinia, N. *Appl. Catal. A: Gen.* **2010**, *378*, 195–201.
23. Markas, A. T.; Hart, J. P. *Analyst* **1995**, *120*, 1029–1045.
24. Kerman, K.; Özkan, D.; Kara, P.; Karadeniz, H.; Özkan, Z.; Erdem, A.; Jelen, F.; Özsöz, M. *Turk. J. Chem.* **2004**, 28, 523–533.
25. Mazloum-Ardakani, M.; Beitollahi, H.; Sheikh-Mohseni, M. A.; Benvidi, A.; Naeimi, H.; Nejati-Barzoki, M.; Taghavinia, N. *Colloids Surf. B* **2010**, *76*, 82–87.
26. Khorasani-Motlagh, M.; Noroozifar, M. *Turk. J. Chem.* **2004**, *28*, 369–378.
27. Mazloum-Ardakani, M.; Ebeahimi Karimi, P.; Naeimi, H.; Mirjalili, B. B. F. *Turk. J. Chem.* **2008**, *32*, 571–584.
28. Raoof, J. B.; Ojani, R.; Beitollahi, H. *Electroanalysis* **2007**, *19*, 1822–1830.
29. Mazloum-Ardakani, M.; Moosavizadeh, S. H.; Sadeghiane, A.; Mashhadizadeh, M. H.; Karimi, M. A. *Turk. J. Chem.* **2010**, 34, 229–240.

30. Laviron, E. *J. Electroanal. Chem.* **1979**, *101*, 19–28.
31. Sharp, M.; Petersson, M.; Edstrom, K. *J. Electroanal. Chem.* **1979**, *95*, 123–130.
32. Bard, A. J.; Faulkner, L. R. *Electrochemical Methods: Fundamentals and Applications*, 2nd ed., Wiley, New York, 2001.
33. Galus, Z. *Fundamentals of Electrochemical Analysis*, Ellis Horwood, New York, 1976.
34. Safavi, A.; Maleki, N.; Moradlou, O.; Tajabadi, F. *Anal. Biochem.* **2006**, *359*, 224–229.
35. Yao, H.; Sun, Y.; Lin, X.; Tang, Y.; Huang, L. *Electrochim. Acta* **2007**, *52*, 6165–6171.
36. Jiao, S.; Li, M.; Wang, C.; Chen, D.; Fang, B. *Electrochim. Acta* **2007**, *52*, 5939–5944.
37. Lin, X.; Zhuang, Q.; Chen, J.; Zhang, S.; Zheng, Y. *Sens. Actuators B* **2007**, *125*, 240–245.
38. Gilmartin, M. A. T.; Hart, J. P. *Analyst* **1992**, *117*, 1299–1303.